

## **Electronic Supplementary Information (ESI)**

### **Multifunctional lanthanide metal-organic framework supported by Keggin type polyoxometalates**

Wen-Hua Zhu, Min Zeng, Juan Wang,\* Chen-Yang Li, Li-Hong Tian, Jia-Cheng Yin,  
and Yu-Kun Liu

*Hubei Collaborative Innovation Center for Advanced Organic Chemical Materials,  
Ministry-of-Education Key Laboratory for the Synthesis and Application of Organic  
Functional Molecules, College of Chemistry and Chemical Engineering, Hubei  
University, Wuhan 430062, PR China.*

## Experimental Section

### Reagents and Physical Measurements

All analytical chemical reagents were obtained from commercial sources and used directly without further purification. IR spectra were recorded in the 4000–400  $\text{cm}^{-1}$  region using KBr pellets on a Nicolet 170SXFTIR spectrometer. The UV/Vis spectra for solution samples were obtained on a Lambda 35 spectrophotometer in the range 200–800 nm. C, H and N microanalyses were carried out with a Perkin-Elmer 240 elemental analyzer. Near-infrared luminescence measurements were performed with a FLS-20 spectrophotometer (Edinburgh Instruments Ltd.). Thermogravimetric analyses (TG) were recorded on a U.S. Perkin Elmer Company Diamond TG/DTA thermal analyzer under a nitrogen atmosphere with a heating rate of 20  $^{\circ}\text{C}/\text{min}$  between ambient temperature and 800  $^{\circ}\text{C}$ . The power XRD data were collected on a D/MAX-IIIC (made in Japan) diffractometer with Cu  $K\alpha$  ( $\lambda = 1.5418 \text{ \AA}$ ) over the  $2\theta$  range of 5–80 $^{\circ}$  at room temperature. The nitrogen adsorption isotherms were measured by a Micromeritics ASAP 2020 instrument at 77 K.

Absorption experiment of dye molecules: a suspension of powder complex (50 mg) in 100 mL fresh aqueous solution of RhB (10  $\text{mg}\cdot\text{L}^{-1}$ , 15  $\text{mg}\cdot\text{L}^{-1}$ , 20  $\text{mg}\cdot\text{L}^{-1}$ ) were first stirred for 5 min, and shaken at a constant rate. At given irradiating intervals (30 min), a series of suspension of a certain volume (4 ml) were collected and centrifuged through a Shanghai TGL-16C centrifuge to remove suspended particles, and the filtrate was analyzed on Shanghai 722N vis-spectrophotometer. The concentrations of the dye molecules were characterized by the absorbance at 554 nm, which directly relates to the structure change of its chromophore.

Static magnetic measurements including temperature-dependent magnetic susceptibility in the range 2–300 K, and field-dependent magnetization at 2 K of **1** were carried out on a Quantum Design MPMS-XL SQUID magnetometer. Alternating current susceptibilities of **1** were also measured using a Quantum Design MPMS-XL SQUID magnetometer. All of the magnetic measurements were performed on polycrystalline samples tightly packed and sealed with a capsule to avoid the anisotropic orientation. Diamagnetic corrections were made with Pascal's constants for all the constituent atoms.

### X-ray Crystallography

Suitable single crystal was selected and mounted in air onto thin glass fibers. The crystallographic data were collected at 296 (2) K on a Bruker SMART APEX CCD fine-focus sealed tube diffractometer with graphite monochromatic Mo- $K\alpha$  ( $\lambda = 0.071073 \text{ nm}$ ) radiation. Data reductions were performed with the SAINT software and absorption corrections were handled by the SADABS software packages, respectively.<sup>1</sup> The crystal data of the complex were solved by direct methods and refined by a full-matrix least-squares method on  $F^2$  using the SHELXL-97 crystallographic software.<sup>2</sup> The N atom of L (type II) ligand is disordered with a neighboring C atom at two positions as shown in Fig. 1. The crystallographic data and structure determination parameters for **1** are listed in Table S1. Selected bond angles and distances are displayed in Table S2.

**Synthesis and IR Spectra of  $\text{H}_3[\text{Nd}_8(\text{L})_{12}(\text{H}_2\text{O})_8] \cdot (\text{SiW}_3\text{W}^{\text{VI}}_9\text{O}_{38}) \cdot (\text{H}_2\text{O})_{10}$  (**1**)**

A mixture of  $\text{Nd}(\text{NO}_3)_3 \cdot 6\text{H}_2\text{O}$  (0.4383 g, 1.00 mmol),  $\text{H}_2\text{L}$  (0.3342 g, 2.00 mmol), silicotungstic acid ( $\text{H}_4\text{SiW}_{12}\text{O}_{40}$ ) (0.1439 g, 0.50 mmol) in deionized  $\text{H}_2\text{O}$  (35 mL) was adjusted to  $\text{pH} = 2.0$  with 1.00 M sodium hydroxide at room temperature. Then the resulting solution was transferred into a 50 mL capacity Teflon-lined stainless-steel vessel and heated at  $160\text{ }^\circ\text{C}$  for 3 days. After cooling to room temperature overnight, beautiful violet block-shaped crystals of **1** were obtained, filtered off, washed with distilled water and then washed for three times by N, N-Dimethylformamide (DMF). Anal. (%) Calcd for  $\text{C}_{84}\text{H}_{72}\text{N}_{12}\text{O}_{104}\text{Nd}_8\text{SiW}_{12}$ : C, 16.01; H, 1.14; N, 2.67. Found: C, 16.31; H, 1.56; N, 2.37.

IR (KBr,  $\text{cm}^{-1}$ , Fig. S1): The broad band around  $3433\text{ cm}^{-1}$  in the spectrum corresponds to the characteristics of the water molecules<sup>3</sup>. The broadness of  $\nu_{\text{O-H}}$  shows the existence of the hydrogen bonds involving water molecules in the complex. The characteristic bands of dicarboxylate groups at  $1611$ ,  $1581\text{ cm}^{-1}$  and  $1396$ ,  $1366\text{ cm}^{-1}$  are attributed to the asymmetric stretching and the symmetric stretching, respectively. The separations ( $\Delta$ ) between the two peaks of  $\nu_{\text{asym}}$  (COO) and  $\nu_{\text{sym}}$  (COO) are both  $215\text{ cm}^{-1}$ , which are attributed to the co-existence of both bridging and chelate modes of the carboxylate groups in compound **1**.<sup>4</sup> Besides, the characteristic peaks of pyridine appear at  $1484\text{ cm}^{-1}$  ( $\nu_{\text{C=N}}$ ),  $1036\text{ cm}^{-1}$  ( $\delta_{\text{CH}}$ ) and  $804\text{ cm}^{-1}$  ( $\gamma_{\text{CH}}$ ). In addition,  $[\text{SiW}_3\text{W}^{\text{VI}}_9\text{O}_{38}]^{3-}$  has four distinctive peaks:  $976$  (W-Ot),  $926$  (Si-Oa),  $879$  (W-Ob-W),  $766\text{ cm}^{-1}$  (W-Oc-W),<sup>5</sup> while the W-Ot peak vibrations show red shifts from  $974$  to  $976\text{ cm}^{-1}$ , the Si-Oa peak shifts from  $915$  to  $926\text{ cm}^{-1}$ , the W-Ob-W peak shifts from  $873$  to  $879\text{ cm}^{-1}$ , and the W-Oc-W peak shifts from  $730$  to  $766\text{ cm}^{-1}$ . These results indicate that the polyoxometalates in the complex still retain the basic Keggin structure, but they are distorted due to the effects of restricted space. This is in accordance with the results of the single-crystal X-ray diffraction studies.

- 1 G. M. Sheldrick, *SADABS, Program for Siemens area detector absorption correction*, University of Göttingen, 1996.
- 2 (a) G. M. Sheldrick, *SHELXS97, Program for the solution of crystal structures*, University of Göttingen, Germany, 1997; (b) G. M. Sheldrick, *SHELXS97, Program for the refinement of crystal structures*, University of Göttingen, Germany, 1997.
- 3 H. Zhang, L. -Y. Duan, Y. Lan, E. -B. Wang and C. -W. Hu, *Inorg. Chem.*, 2003, **42**, 8053–8058.
- 4 (a) K. Nakamoto, *Infrared and Raman Spectra of Inorganic and Coordination Compounds*; John Wiley & Sons: New York, 1986; (b) C. -H. Li, K. -L. Huang, Y. -N. Chi, X. Chi, Z. -G. Han, L. Shen and C. -W. Hu, *Inorg. Chem.*, 2009, **48**, 2010–2017.
- 5 A. Kaur, G. Hundal, and M. S. Hundal, *Cryst. Growth Des.*, 2013, **13**, 3996–4001.

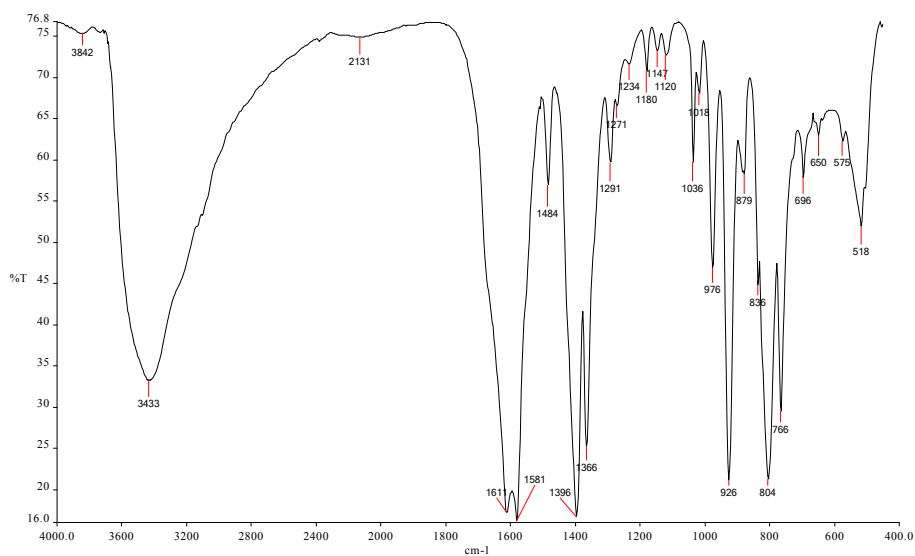


Fig. S1 IR spectrum of compound 1.

Table S1 Crystallographic data for the compound 1

<b>1</b>	
Empirical formula	$C_{84}H_{72}N_{12}O_{104}SiW_{12}Nd_8$
Formula weight	6301.74
Crystal system	monoclinic
Space group	$P2(1)/m$
$a$ [Å]	17.353(2)
$b$ [Å]	30.453(3)
$c$ [Å]	17.511(2)
$\alpha$ [°]	90
$\beta$ [°]	119.547(2)
$\gamma$ [°]	90
Volume [Å <sup>3</sup> ]	8050.3(15)
$Z$	2
$D_c$ [g cm <sup>-3</sup> ]	2.600
$\mu$ (Mo $K\alpha$ ) [mm <sup>-1</sup> ]	11.173
$F(000)$	5748
Crystal size, mm <sup>3</sup>	0.28×0.24×0.22
$\theta_{min}, \theta_{max}$ [°]	1.337, 27.449
Total reflections collected	41641
Uniq reflections ( $R_{int}$ )	18633 (0.0061)
No. of refined parameters	1060
$R1, wR2$ [ $I \geq 2\sigma(I)$ ]	0.0355, 0.1090
$R1, wR2$ (all data)	0.0487, 0.1343
Goodness of fit	1.034

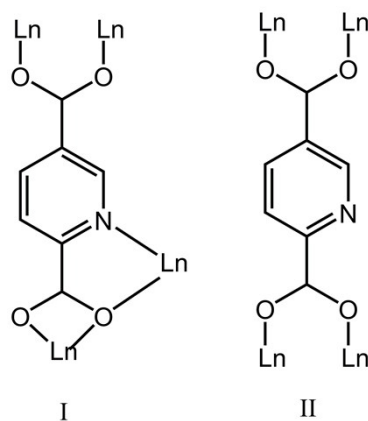
**Table S2** Selected bond lengths (Å) and angles (°) for **1**

Nd(1)-O(1)	2.576(5)	Nd(1)-O(1w)	2.484(5)
Nd(1)-O(8)#5	2.475(5)	Nd(1)-O(9)	2.647(5)
Nd(1)-O(10)	2.567(5)	Nd(1)-O(13)	2.472(5)
Nd(1)-O(15)#3	2.483(5)	Nd(1)-O(23)#4	2.435(5)
Nd(1)-N(2)#3	2.702(6)		
Nd(2)-O(2)	2.696(5)	Nd(2)-O(2w)	2.449(5)
Nd(2)-O(3)	2.352(5)	Nd(2)-O(10)	2.444(4)
Nd(2)-O(12)#4	2.419(4)	Nd(2)-O(14)	2.418(4)
Nd(2)-O(17)	2.673(5)	Nd(2)-O(18)	2.509(5)
Nd(2)-N(1)	2.669(5)		
Nd(3)-O(3w)	2.550(5)	Nd(3)-O(4)	2.501(5)
Nd(3)-O(5)	2.381(4)	Nd(3)-O(11)#4	2.422(4)
Nd(3)-O(18)	2.519(5)	Nd(3)-O(20)#2	2.454(5)
Nd(3)-O(21)	2.660(5)	Nd(3)-O(22)	2.616(4)
Nd(3)-N(3)	2.670(5)		
Nd(4)-O(4w)	2.526(5)	Nd(4)-O(6)	2.483(4)
Nd(4)-O(7)	2.412(5)	Nd(4)-O(15)#2	2.552(5)
Nd(4)-O(16)#2	2.643(5)	Nd(4)-O(19)#2	2.411(4)
Nd(4)-O(22)	2.428(5)	Nd(4)-O(24)#6	2.445(5)
Nd(4)-N(4)	2.717(6)		

Symmetry codes: #1 x, -y+3/2, z, #2 -x+1, -y+2, -z+1, #3 -x+2, -y+2, -z+1, #4 -x+1, -y+2, -z, #5 x+1, y, z, #6 -x, -y+2, -z, #7 x-1, y, z, #8 x, -y+1/2, z.

**Table S3** The bond valence sum (BVS) calculations of the five-coordinate W centers for **1**

Atom	Bond	Bond distances (Å)	BVS	Assigned oxidation state
W6	W6-O6A	1.685	4.78	+5
	W6-O12A	1.880		
	W6-O12A	1.880		
	W6-O13A	1.978		
	W6-O23A	2.313		
W7	W7-O7A	1.675	4.55	+5
	W7-O8A	1.830		
	W7-O13A	2.279		
	W7-O14A	1.849		
	W7-O23A	2.431		



**Scheme S1** Coordination modes of L (type I and II) ligands in complex 1.

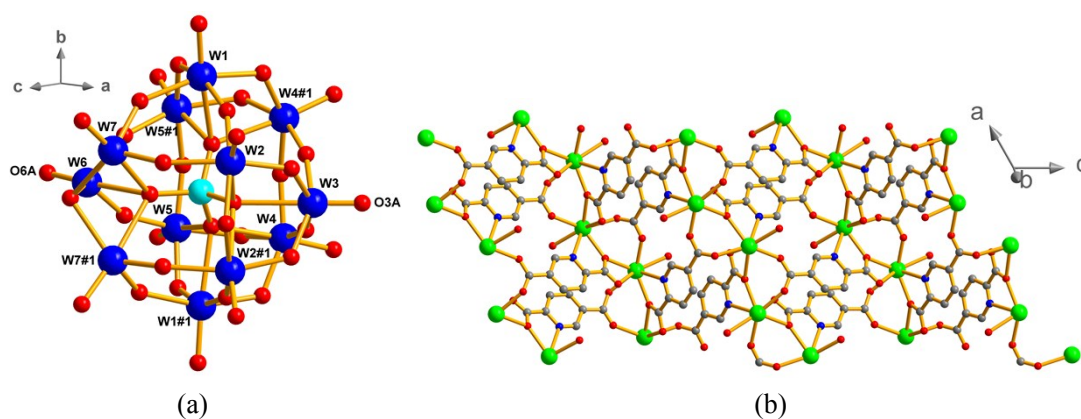


**Fig. S2** (a) Structural view of the POM anion. (b) The 2D structure along *ac* plane.

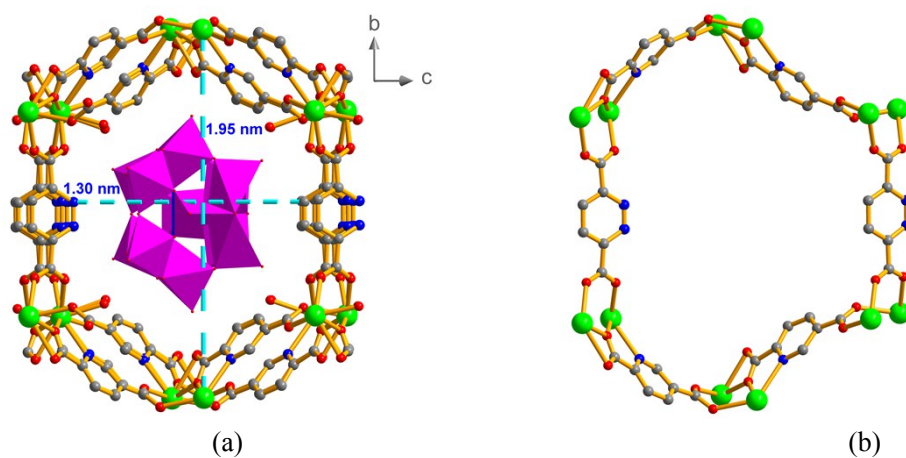


**Fig. S3** (a) View of dimensions of the hexagonal window. (b) View of the metallamacrocycle.

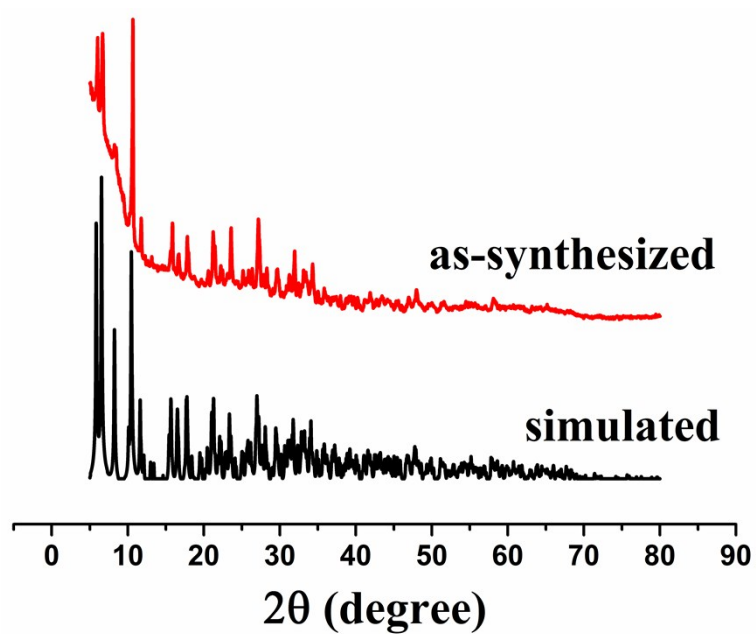


Fig. S4 The PXRD patterns for 1 in the range of 5 to 80 degrees.

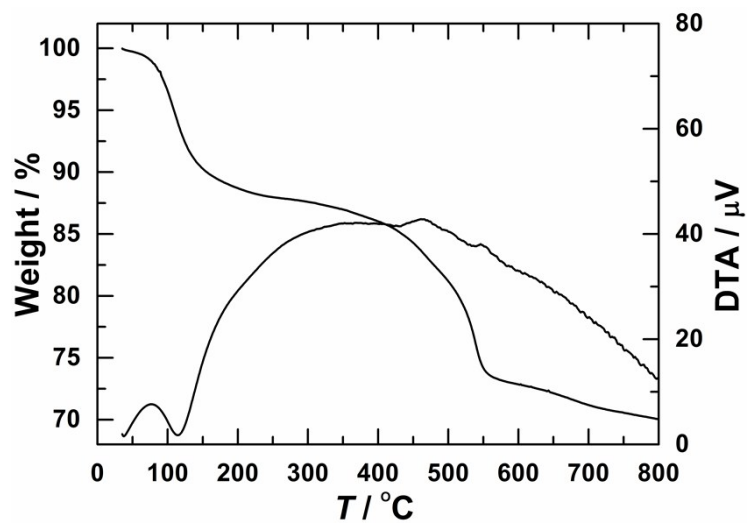


Fig. S5 The TG-DTA curves for complex 1.

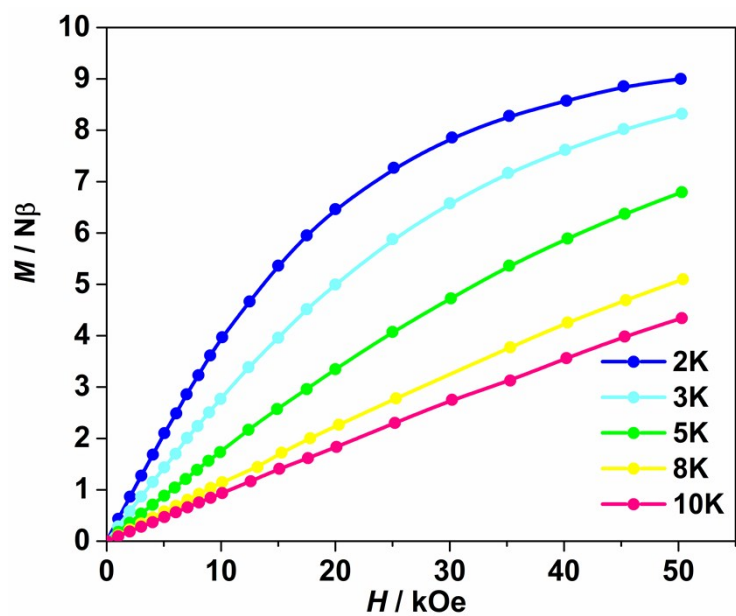


Fig. S6 Field dependence of the magnetization for **1** at 2.0 K.

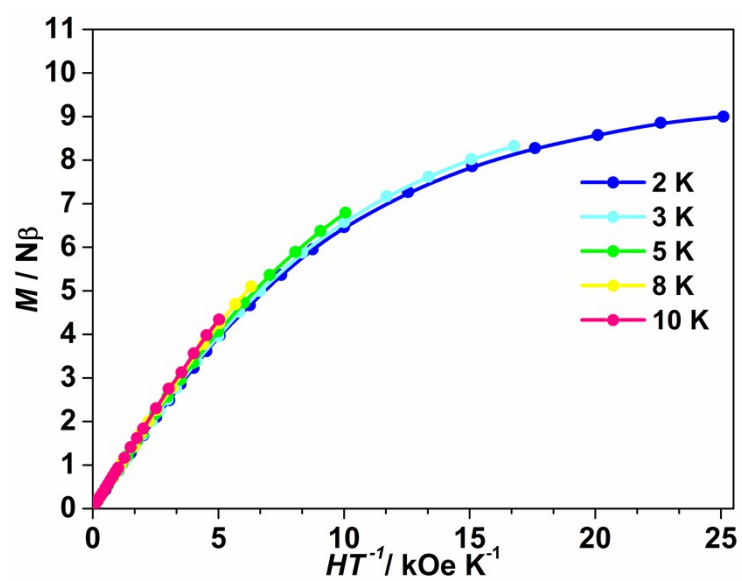
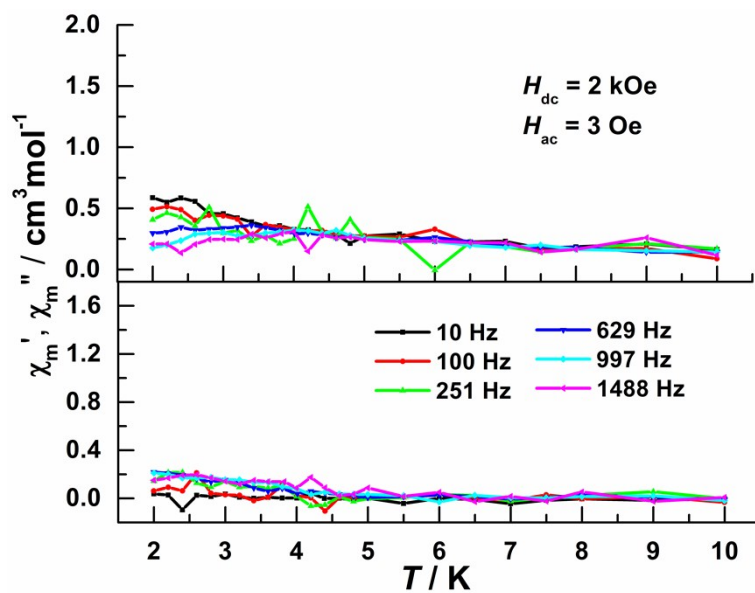
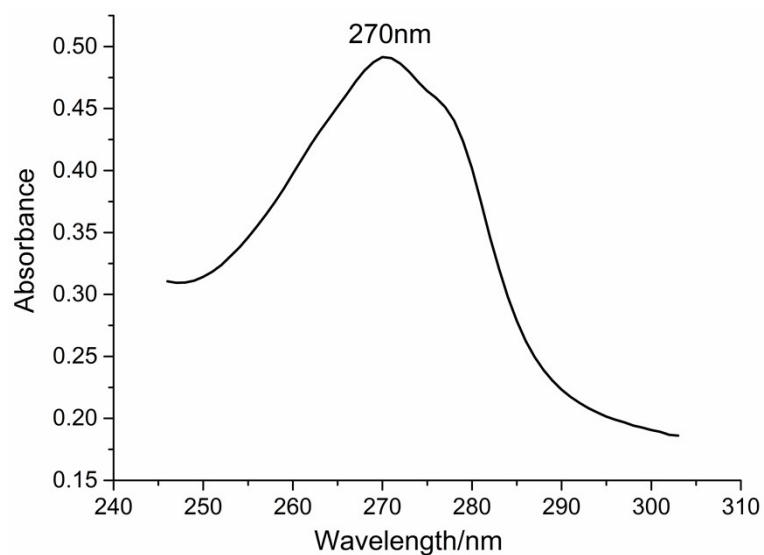


Fig. S7 Field dependence of the magnetization for **1** at 2.0 K.





**Fig. S8** Temperature dependence of the real (top) and imaginary (bottom) components of ac susceptibilities of **1** under a 2 kOe dc field.



**Fig. S9** The UV/Vis spectrum of compound **1** in solution.

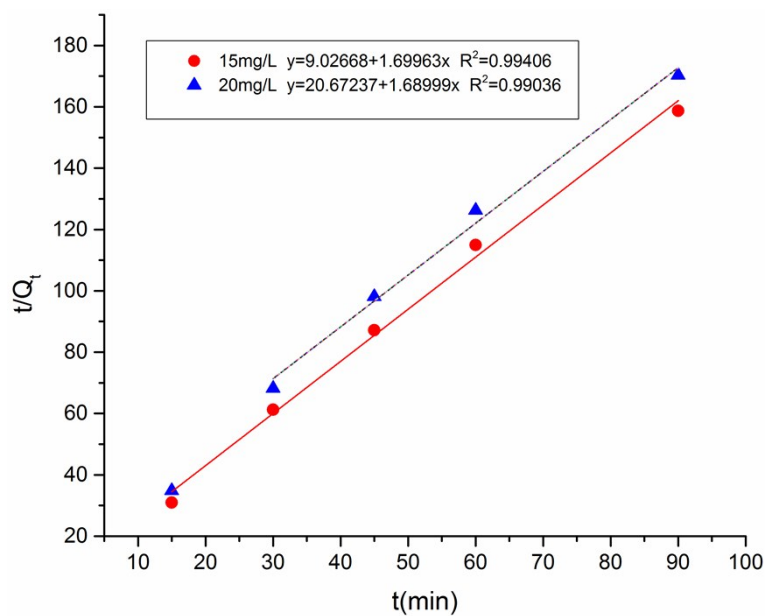


**Fig. S10** Pseudo second-order adsorption of RhB dye molecules onto powder **1** at the concentrations of  $15 \text{ mg}\cdot\text{L}^{-1}$  and  $20 \text{ mg}\cdot\text{L}^{-1}$  in solution.